

# INFLUENCE OF THE SURFACE TEMPERATURE ON LIBS ANALYZES IN SIMULATED MARTIAN CONDITIONS

V. Lazic<sup>(1)</sup>, I. Rauschenbach<sup>(2)</sup>, S. Jovicevic<sup>(3)</sup>, E. K. Jessberger<sup>(2)</sup>, R. Fantoni<sup>(1)</sup>, M. Di Fino<sup>(1)</sup>

<sup>(1)</sup>ENEA, FIS-LAS, Via. E. Fermi 45, 00044 Frascati (RM), Italy, [lazic@frascati.enea.it](mailto:lazic@frascati.enea.it)

<sup>(2)</sup>Institut fuer Planetologie, Westfaelische Wilhelms-Universitaet, Muenster, Germany

<sup>(3)</sup>Institute of Physics, 11080 Belgrade, Pregrevica 118, Serbia

## ABSTRACT

We applied Laser Induced Breakdown Spectroscopy (LIBS) on moist soil/rock samples in simulated Martian conditions. For the first time, the LIBS signal behavior as a function of the surface temperature was studied, here in the range from +25°C to -60 °C and at pressure of 7 mbar. We observed the strong signal oscillations below 0°C with different negative peaks, whose position, width and magnitude depend on the surface roughness. We attribute such a signal behavior to the presence and phase transitions of supercooled water inside the surface pores. The LIBS signal decrease was always registered close to 0°C, corresponding to the freezing/melting of normal hexagonal ice. Comparative measurements were performed on a frozen water solution. A large depression of the LIBS intensity was observed close to -50°C. Ablation rates and plasma parameters as a function of the sample temperature are also discussed, and their consequences for in-situ analyses.

## 1. INTRODUCTION

ExoMars, the future mission to Mars of ESA will include a LIBS instrument to analyze the elemental composition of the Martian surface materials [1-2]. The instrument should perform the measurements with the external temperature in the range from +30°C to -60°C. Removal of the surface debris and ice via laser ablation is also planned.

Spacecraft- and Earth-based telescopic measurements mapped water vapor and ice-clouds in the Martian atmosphere [3]. The water vapor is transported by winds; it can diffuse into the subsurface and becomes water ice at high latitudes. Spectroscopic measurements of sunlight reflected from the Mars surface indicate that a certain amount of water adsorbed by soil. Hydrogen was mapped within near surface regions at high latitudes and on the surface in the polar regions. Observations from the gamma ray spectrometer on Mars Odyssey spacecraft shows the ice presence with concentrations above 70% at 60° latitude and even higher near poles and smaller presence of unstable ice closer to equator [4]. Therefore, in LIBS analyses of Martian soils, the presence of water and ice should be taken into account.

The Martian atmosphere is composed mainly of CO<sub>2</sub> and NASA's Viking Landers registered average daily pressures between 6.8 mbar and 10.8 mbar, higher during summer and also depending on the site. At a pressure of 6 mbar, water has the triple point at 0.01 °C. Below this pressure, there is a direct transformation of water vapor into ice and vice-versa, while above this pressure a water phase also can exist.

Although the characteristics of water and of its solid phases were extensively studied, a complex behavior of water is not yet fully understood [5]. Hexagonal ice (Ih) is normally formed at low pressures and is stable from about -200°C to 0°C [5]. On the other hand, cubic ice Ic is metastable and can be formed by condensation of water vapor at temperatures less than -80°C [5] or at somewhat higher temperatures (below -38°C) from condensation of small droplets (~6 µm diameter or less). Ice Ic is often found in freezing confined (porous) aqueous systems [6-7]. By warming, ice Ic transforms into ice Ih over a wide temperature range, from about -110°C K to -30°C K [8]. By cooling free water below 0°C, normally ice Ih is formed. However, if water is cooled carefully, the liquid form can exist down to about -40°C, so called temperature of homogeneous nucleation Th [5, 9]. On rock/soil surfaces and in larger sample structures water can be considered as a bulk, not confined water.

When considering water/ice on the soil/rock surfaces and inside their pores, different effects must be taken into account. External water on the surface nucleates to the normal form of hexagonal ice. Unfrozen supercooled water films can exist at subzero temperatures, particularly at interfaces with soil particles or at grain boundaries [6-7, 10-11]. The fraction of unfrozen water below 0°C depends on sizes and shapes of the pores and grains, then on impurity concentrations and local environment (pressure and temperature) [11-12]. In presence of salts, an existence of supercooled water in soils was measured down to -40°C [12]. Freezing of free pore water, also in soils [11], leads to the formation of a defective form of cubic ice (Ice-I) that is intermediate between Ih and Ic. The melting point of small ice crystals is inversely proportional to the crystal size i.e. pore size of the material, and there are indications that an interfacial supercooled water on corrugated pore walls could exist even below -80°C [7]. Hexagonal surface ice, pore ice

and supercooled water have different physical properties [5, 13-14], such as thermal conductivity, density, diffusion coefficient, viscosity, absorption coefficient, etc. All these characteristics affect the laser ablation and thus the LIBS signal. While surface ice, if present as a thin layer, can be removed by a certain number of laser shots before starting the actual LIBS measurements, water/ice inside pores is a part of the analyzed soil/rock. The LIBS technique allows rapid and multi-elemental in-situ measurements in different surroundings [15]. Sample preparation is not required; the measurements are without contact thus excluding any sample contamination. The laser pulses can be also used to remove an external surface layer prior to the analyses, and elemental distribution at depth can be measured on a small scale (up to a few millimeters). It is also possible to achieve the LIBS system miniaturization and low power requirements [2]. All this makes LIBS technique very promising for planetary exploration although its sensibility and accuracy are generally lower than for some other techniques, such as ICP-OES.

LIBS analytical capability depends on the overall instrument characteristics, on the acquisition parameters, surrounding atmosphere, interaction geometry and on the surface conditions [16-21]. For given experimental conditions, the signal intensities and the achievable analytical accuracy are further compromised by the so-called matrix effect [15-16, 21-22], as an amount of the ablated material, the plasma characteristics and its stoichiometry are influenced by the physical and chemical properties of the sample. A number of publications report quantitative LIBS analyses in simulated Mars atmosphere at a fixed temperature, obtained by different analytical approaches [19-20, 23-25]. Except [24], these analyses regard relatively dry samples and measurements at room temperature. In [24] the LIBS measurements were performed on soil/ice mixtures at two different temperatures, namely 246 K and 165 K. It was found that the ablation rate, and consequently the signal, is higher for about factor 7 at the higher temperature considered. Such difference was attributed to an increased energy requirement to melt the ice at lower temperature. The preparation procedure of soil/ice mixture probably leads to the hexagonal ice formation and to quite different grain/ice interfaces than what we could expect in nature. Beside [24], only one work reports LIBS analyses of ice samples [26] and it deals with trace elements in fixed experimental conditions (temperature).

Given this background, we studied the dependence of LIBS signals on different types of soils and rocks in simulated Martian atmosphere, as a function of the sample temperature in the range from 25°C to -60°C. Both cooling and heating cycles were applied on the samples. The rock fragments had different grades of the surface polishing. During ablation at a single sample point, the spectrum was registered after each laser shot, allowing to eliminate signals from possible surface ice

and to distinguish it from the soil containing pore ice or supercooled water. For comparison, temperature dependent measurements were also performed on a frozen water solution. On one soil sample, the whole spectra were recorded at different temperatures and the change of the plasma parameters with the temperature was also examined.

## 2. EXPERIMENTAL

### 2.1. Laboratory set-up

The LIBS instrument here used is laboratory equipment and does not represent a prototype for Mars exploration. The laser source is an Nd:YAG from Quanta System (Handy) operated at 1064 nm. The laser pulse width is 8 ns and repetition rate is 10 Hz. The laser beam was passed through a 50 mm diameter aluminum pierced mirror and focused onto the sample surface by a quartz lens with 250 mm focal length. The spot size on the sample was of 170-240  $\mu\text{m}$  diameter, depending of the laser energy.

The vacuum chamber, equipped with a 50 mm diameter quartz window, contains a rotating sample holder that can be cooled with liquid nitrogen. The holder can accept up to six samples in pellets. The temperature of the sample surface was measured indirectly, by using the same sample type with similar thickness, placed in a contact with a thermocouple type K. The temperature was read directly by HP 3852A Data Acquisition/control unit.

In this work, the laser energies delivered to the sample were 12.5 mJ or 70 mJ that lead to fluencies of about 14  $\text{J}/\text{cm}^2$  and 40  $\text{J}/\text{cm}^2$  respectively. The latter fluence corresponds to a lower power density limit of 5  $\text{GW}/\text{cm}^2$ , initially specified by ESA. However, we considered also a lower fluence i.e. power density, as the specified value from above could be a subject of revision in view of further volume/ weight reduction of the LIBS system.

Before starting the measurements, the vacuum chamber was evacuated down to 0.01 mbar and then a flux of a laboratory grade  $\text{CO}_2$  was introduced, regulated to keep the gas pressure at 7 mbar. Otherwise, for some measurements we used a mixture of 1 mbar of air and 6 mbar of  $\text{CO}_2$ . Air was introduced in order to allow for water vapor condensation on the sample (see section 3.). The emission from plasma is reflected by the pierced mirror towards a wide-angle collecting optics terminating with a fiber optic bundle. At the exit, the fiber bundle is arranged into an array of 0.1x2.6 mm and mounted on the entrance slit of a 550 mm monochromator (Jobin-Yvon Triax 550). A grating with 1200 grooves/mm was used in all the measurements. At the monochromator exit plane, a gated ICCD (Andor, 1024x256 pixel), recorded the LIBS spectra. The overall equipment is controlled by custom written software routines. The ICCD gain was set to 0 in order to evaluate a use of more compact, non-intensified sensor.

The gate width was chosen to be 5  $\mu$ s, corresponding to the maximum gate width specified by ESA. After initial time-resolved spectral acquisition on soil samples, we obtained maximum Signal-to-Noise Ratio (SNR) when using an acquisition gate delay of 200 ns, thus in all further measurements this value was kept unchanged.

For LIBS signal measurements as a function of the sample temperature, the monochromator was kept at a fixed wavelength (283 nm) and we applied 20-50 laser shots at fixed points: 20 on ice sample, 30 on pressed soil samples and 50 on the rock samples. Such choice was guided by different ablation rates among these samples and an intention to minimize the crater effects. A spectrum that was acquired at each laser shot was stored separately inside a single file for that one measurement (one sample at a certain temperature). This approach allows monitoring of the shot-to-shot variations of the spectral intensities, and is also useful for rejecting the spectra affected by an eventual crater effect, which can cause the signal reduction [27]. Most importantly in our studies, it allows for post-experimental elimination of a certain number of the first laser shots. By summing only those spectra that were obtained after a number of initial laser shots, we eliminate a contribution of possible surface ice to the overall signal.

When acquiring full spectra of the samples, the signal was simply accumulated over 20 laser shots.

## 2.2. Samples

We analyzed rock samples considered as Martian analogues, then certified soils samples with different matrices, and ice samples.

The rocks analyzed are belonging to the group of andesites or basalts. The andesite sample originates from the Eifel region in South-West Germany, known for its volcanic activity in the Tertiary. From SEM-EDX sample characterization we found out that the main constituent is silica (about 43%). The basalt sample originates from the Vogelsberg Mountains in central Germany with a formerly active shield volcano. It contains about 45% of silica. The sample surfaces were prepared by three different grades of polishing (Fig. 1).

The examined soil samples are certified reference materials, chosen in view of generating of the calibration graphs. The samples were pressed into pellets by applying equivalent weight of 20 t.

The ice sample was prepared from pure milli-Q water where  $MgSO_4$  was properly added to obtain a solution corresponding to 50 mg/l of Mg. This element has some strong emission lines and normally is present in soils and rocks. The solution was poured in equal quantities onto two identical glass dishes; one of them was used for LIBS analyses and another for the temperature measurements. These samples were slowly cooled down below 0°C in order to obtain homogeneous ice nucleation and consequently a smooth surface.

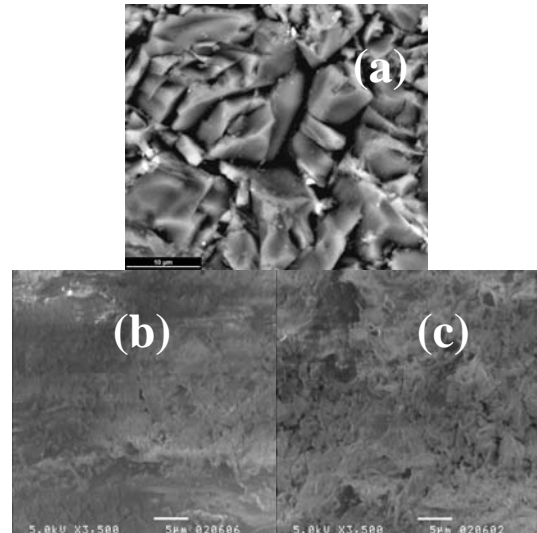


Fig. 1: SEM images of andesite rock surface after (a) polishing #1; (b) polishing #2 and (c) polishing #3.

## 3. RESULTS

The measurements of the LIBS signal as a function of the sample temperature were performed in the limited spectral range 270-295 nm. This spectral interval contains one atomic line each from Si and Mg, different ionic Mg lines useful for determining the ratio  $Mg/Mg^+$  in the plasma and an intense ionic  $Fe^+$  multiplet. The emission lines of these three elements were detectable on all the analyzed rock and soil samples.

### 3.1. Rock samples

First, we studied the signal behavior on the andesite rocks sample that had been polished #1 (Fig. 1a), i.e. corresponding to roughest surface considered. The measurements were performed in 1 mbar air pressure plus 6 mbar of  $CO_2$ . The presence of air was aimed to allow for water condensation inside the pores. The cooling cycle was very slow, about 10 °C/hour, to allow the measurements with a high temperature resolution. In order to remove the contribution from eventual surface ice, the spectra registered with the first 10 shots were in following discarded by software, while those obtained with the successive 40 shots were summed and further analyzed. The measured line spectral intensities are practically constant down to 5°C (Fig. 2a). Then they undergo a strong reduction, of about 50%, for the temperatures between +3°C and +4°C. With such slow cooling rates, we estimated experimentally the temperature error of  $\pm 1^\circ C$ , caused by an indirect temperature determination on the LIBS analyzed sample. One possible reason for here observed LIBS signal depression can be searched in water boiling - at pressure of 7 mbar the boiling point of pure water is +2°C, which is consistent with the measured sample temperature taken with the error. In addition, water containing impurities, as it is case here due to a partial dissolution of some sample constituents, has a higher

boiling point than pure water, but an amount of its change is difficult to evaluate here.

With further sample cooling the signal recovers almost immediately and then drops sharply at 0°C. Between -5°C and -15°C the signal is almost constant and about 10 times lower than the average intensity measured above 5°C. We attribute that broad negative peak to the presence of supercooled water inside the surface pores of the rock. Further lowering of the sample temperatures leads to partial signal recovery with respect to the room temperature, probably due to the then completed freezing of supercooled water inside pores [11]. The wide minimum peak immediately below 0°C is analogue to the observed interfacial ice melting on amorphous silica [10], which was used to simulate rock-water interfaces. A comparison of spectra obtained at the temperatures of +10°C and -10°C is shown in Fig. 3. It is clear that measurements at the low temperature, corresponding to the maximum signal depression (Fig. 2a) leads to an important loss of analytical information as many emission lines now can no more be distinguished from the noise. The temperature dependence of the continuum spectral component (not shown), which is in general correlated to the ablation rate [26], has the analogue features as the intensities of the emission lines. Accordingly, it seems that the observed signal reduction in a wide interval below zero is mainly related to the decrease of the ablation rate.

The ratio of Mg<sup>+</sup> peak at 280.3 and Mg peak at 285.2 nm remains practically constant for temperatures down to about -20°C (not shown). Below this temperature, the ionic to atomic intensity ratio increases and at -40°C it is about 30% higher than an average value at higher temperatures. As the ionic emission increases with the plasma temperature and/or with lowering of the plasma electron densities, we hypothesize that in this range the plasma parameters changed.

The surface of the same andesite sample was then treated with emery (polishing #2, Fig. 1b). Now, the surface exhibits the large scratching left by the abrasive grains, but inside the same, the pore sizes although not uniform, are visible smaller than in the previous case. In order to accelerate the measurements, the cooling rate was increased to about 25°C per hour. Starting at room temperature, from one measurement to another the signal oscillates less than ±7% of the average value (Fig. 2b). A signal depression, about 55% of its maximum value, was observed close to 0°C where the formation of normal, disordered ice is expected inside scratching and larger pores. Below 0°C, more violent signal oscillations as a function of the temperature are registered. A number of small negative peaks are attributed to different dimensions of the surface pores, each one having its specific and different temperature of water-to-ice transition [7-8, 13].

When the same rock sample was polished by a diamond substrate with a finer grain size (polishing #3, Fig. 1c) 1), the surface resulted rather uniform except in some points due to the inclusions. The LIBS measurements

were repeated different times, both during the cooling and heating cycles, with different cooling/heating rates (15-25 °C per hour). After the initial cooling cycle performed down to -30°C with air entrance (1 mbar), followed by heating, the measurements started but the thermal cycle was expanded down to -55 °C by filling the chamber only with CO<sub>2</sub> (7 mbar). In presence of air, it was not possible to reach such low temperature as the pressure becomes unstable around -40°C.

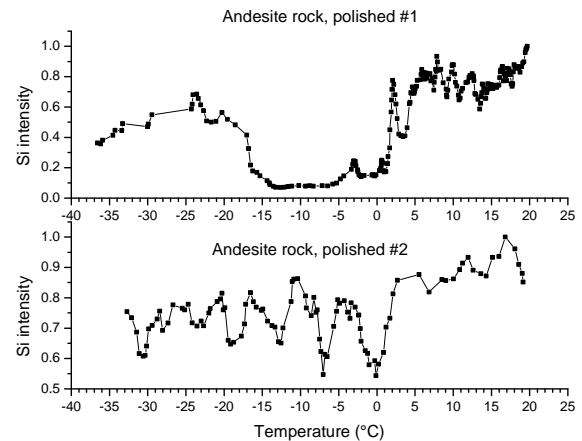


Fig. 2: Normalized Si peak intensity from Andesite rock sample for two surface polishing; cooling cycle, 14 J/cm<sup>2</sup>.

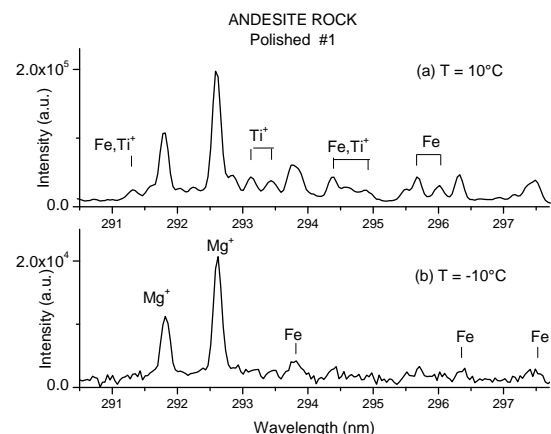


Figure 3: Example of spectra obtained on andesite rock, polishing #1, for two surface temperatures; accumulation by 40 laser shots, cooling cycle, 14 J/cm<sup>2</sup>.

Now, with the changed surface morphology, besides some oscillations, the signal remains practically constant in the whole temperature range except one very deep (about 50% of the initial value) and narrow negative peak about -10 °C (Fig. 4). The same peak appears also when the laser fluence on the sample was increased from 14 J/cm<sup>2</sup> to 40 J/cm<sup>2</sup>. As these measurements were performed on different areas of the sample, the described signal behavior could be attributed to the presence of rather uniform surface with smaller pore size than in the first case (Fig. 1a). On a

basalt rock sample, prepared in the same way (polishing #3), the negative peak around  $-10\text{ }^{\circ}\text{C}$  was again observed thus confirming that its appearance is mainly determined by the surface preparation.

In all the cases, the signal depression close to zero temperature is very low, thus indicating a very low fraction of the hexagonal ice formation. Here, we considered the LIBS signal after applying first 10 laser shots, which is assumed to remove the surface ice. Thus the contribution of the hexagonal ice and the corresponding signal depression close to  $0^{\circ}\text{C}$  can come only from a relatively large pores overfilled with water, which seems to be almost absent on this well polished sample. At lower laser fluence applied, the cooling and heating cycles were sufficiently slow to distinguish clearly another negative peak around  $-48^{\circ}\text{C}$ , with very strong signal reduction, up to about 80%. A similar negative peak as here was observed by Differential Scanning Calorimetry (DSC) applied on mesoporous silica materials [6]. This negative peak was registered independently of pore sizes and it was hypothesized that such a behavior is inherent to the boundary layer of water at silica surface. Different experimental techniques show evidence for some kind of thermodynamic transition of supercooled water at about  $-49^{\circ}\text{C}$  [9, 28-29]. Although the reason for this critical behavior is not yet completely clear, it has been proposed that at this temperature the supercooled water, which can exist also at these temperatures and particularly at corrugated surface of pore wall [7], changes from its normal liquid structure to an amorphous hydrogen-bonded network. The phase transition of supercooled water can be a possible explanation of the observed LIBS signal depression at this temperature.

In the heating cycle, the measured signal clearly drops above zero, for about 30% and this was attributed to melting of hexagonal ice inside the larger, overfilled pores.

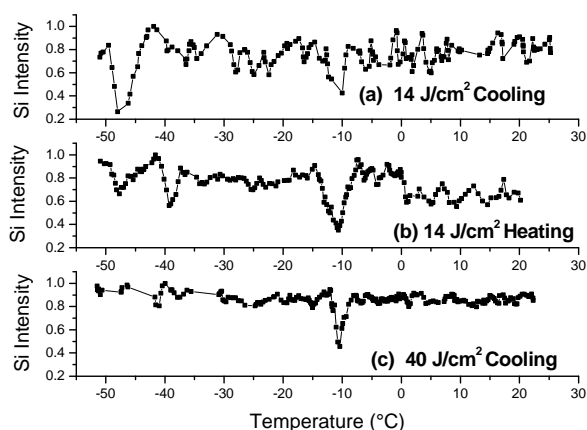


Figure 4: Normalized LIBS Si peak intensity (288.2 nm) on andesite rock after polishing #3 as a function of the surface temperature, accumulated by 40 laser shots and after applying 10 initial cleaning shots

The obtained LIBS signal dependency on the sample temperature measured on the andesite rock polished #1 or #3, which have better defined surface structure, is quite similar to the results reported by DSC for materials with well defined pore dimensions [6-7]. In such measurements, the phase transition is characterized by a discontinuity of the measured thermal conductivity due to latent heat of transition. By comparing LIBS and DSC signal, in the case of laser ablation the absorbed laser energy by coexisting ice-water phase seems to be first used to complete the transition of the ice to the liquid phase and only then to rise the temperature up to the evaporation point, i.e. to ablate the liquid.

It is known that when the sample passes cooling cycle, the freezing temperature can be lower up to  $5^{\circ}\text{C}$  than the melting temperature during heating cycle. The hysteresis behavior is more pronounced for larger pore sizes of the sample [6]. DSC measurements have demonstrated that during heating cycle the measured peaks, related to the phase transitions, do not change position significantly but their intensity increases with the pore filling factor (calculated as volumetric ratio of added water and pore). Differently, during cooling cycle both the peak positions and intensities are dependent on the pore filling factor. We assume that similar influence on the LIBS signal can occur and that this should be further investigated.

### 3.2. Powder samples

On powder samples, which were pressed into pellets, the resulting pore sizes on the surface depend on the initial grain size and on the degree of pressing.

On all the samples examined, a signal depression up to 50% was observed close to  $0^{\circ}\text{C}$ . Below this temperature a series of smaller negative peaks appear, assumed to be due to different and predominant pore sizes and water/ice phase transitions inside.

On the limestone, in the range from  $-5^{\circ}\text{C}$  to  $-32^{\circ}\text{C}$  (the lowest temperature considered) the signal intensity remains low, at about 50% of the value above  $0^{\circ}\text{C}$  (Fig. 5a). Differently, on the Antarctic sediment the maximum values at lower temperatures do not differ appreciable from the values measured above  $0^{\circ}\text{C}$  (Fig. 5b). Also on the reference basalt sample, the maximum signal intensities do not appreciable change with the temperature, but beside the negative peak close to  $0^{\circ}\text{C}$ , another three minima are clearly distinguished: around  $-15^{\circ}\text{C}$ ,  $-25^{\circ}\text{C}$  and  $-40^{\circ}\text{C}$  (Fig. 5c). The negative peak around  $-25^{\circ}\text{C}$  is quite large (about  $7^{\circ}\text{C}$ ) and causes a particularly severe signal drop, for about 70%. Probably, the dominant pore sizes are largely distributed around a diameter corresponding to this freezing temperature of the confined water. A negative peak at  $-40^{\circ}\text{C}$  is quite similar to a peak observed in DSC measurements on cement paste and concrete during cooling cycle [30]. There, this signal drop was attributed to the homogeneous nucleation of unconfined water, occurring at this temperature. An analogue behavior close to  $-40^{\circ}\text{C}$  was also registered by DSC applied on

mesoporous silica during cooling cycle [6], however, in the heating cycle this peak disappears.

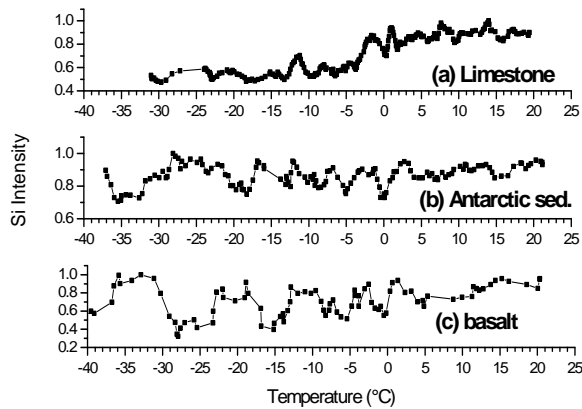


Fig. 5: Normalized Si (288.2 nm) peak intensity on pressed powder samples as a function of the surface temperature, accumulated by 20 laser shots after cleaning by 10 shots; air 1 mbar + CO<sub>2</sub> 6 mbar, cooling cycle, fluence 14 J/cm<sup>2</sup>.

### 3.3. Ice sample

The ice samples were prepared by slow cooling of water solution and LIBS measurements were performed during the heating cycle, starting from the temperature as low as -80°C at pressure of 7 mbar of CO<sub>2</sub>. The applied laser fluence was 40 J/cm<sup>2</sup>. The surface reflectivity was very high as we observed returned beam, refocused on the pierced mirror, which even caused its ablation. The signal was analyzed from Mg<sup>+</sup> peak emission at 280.3 nm. Significant signal oscillations from one measurement to another must be encountered due to not perfectly homogeneous nucleation and to not completely flat surface.

Particularly intense signal changes occur in proximity of the lowest temperature here reached (Fig. 6). At a few temperatures, both the line and continuum intensities are even two orders of magnitude lower than the maximum values obtained during the full heating cycle. Visually observed craters seem very shallow and small in diameter. All these indicate that we operated here close to the ablation threshold. From the repeated measurements on another analogously prepared sample and during different heating cycle, we obtained again a negative peak close to -50°C, which matches the point of anomalous behavior of supercooled water [9]. The same position of a negative peak was observed also in measurements on the andesite rock (Fig.6) where water/ice is confined in small pores and where we hypothesized a phase transition of supercooled liquid. Regarding freezing or heating of bulk water under atmospheric pressure, the existence of supercooled water below temperature for homogeneous nucleation (about -40°C) has not been proved. Presence of salts and impurities in water/ice reduces the freezing temperature and increases the boiling point [12]. Unfortunately, we

have not found detailed studies regarding temperature transformations of bulk or confined ice-water under low ambient pressure as here but above the triple point. We conclude that further studies of ice ablation and corresponding LIBS signal behavior should be performed for temperatures below -40°C.

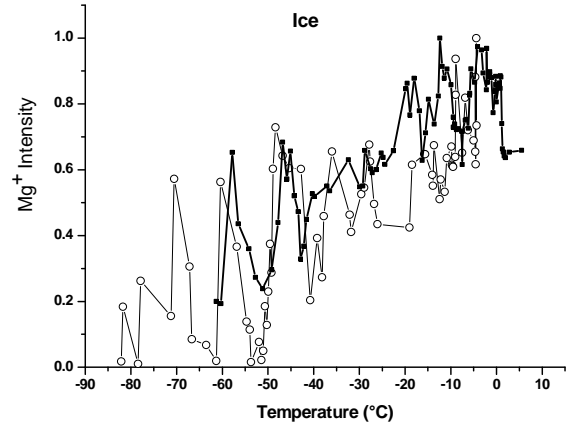


Fig. 6: Repeated measurements of normalized Mg<sup>+</sup> peak intensity (280.2 nm) from frozen water solution containing MgSO<sub>4</sub>: signal accumulation over 30 laser shots, heating cycle, laser fluence 40 J/cm<sup>2</sup>, gas composition: 7 mbar of CO<sub>2</sub>.

Heating the ice sample above -40°C, a progressive signal increase was registered although with oscillations. The reflectivity of ice increases with warming [13] and consequently the absorption coefficient decreases. On the other hand, the heat conductivity of hexagonal ice increases with cooling [14] and accordingly, the ablation threshold becomes higher: From our measurements, it results that the positive influence of low temperature on the ice absorption coefficient is overcome by the increase of the ablation threshold. There is another effect to consider when warming the ice and it is referred to premelting that can occur both on the surface and between crystallite boundaries. At higher temperatures, we observed the ice softening and laser-produced craters become visible larger than the laser spot size. In such conditions, the laser removal of the surface ice would be more efficient than at low temperatures.

### 3.4. Plasma parameters

On a reference basalt sample we acquired full spectra in 240-800 nm range by accumulating 20 laser shots and at six different sample temperatures. The sample was first sprayed with tap water and cooled down to -50°C in presence of 7 mbar of CO<sub>2</sub>. The cooling rate was of about 25°C per hour. The measurements were performed at two laser fluencies (14 and 40 J/cm<sup>2</sup>). Plasma temperature was calculated from the Boltzmann plot applied on different atomic Fe lines that were free of the spectral overlap in the range 380-540 nm. The

plasma density was calculated from Stark broadening of Mg line at 516.7 nm. Previously, the presence of the line self-absorption was excluded by comparing the intensity ratio of the corresponding multiplet with the values from NIST database.

For the higher fluence, the calculated plasma temperatures for different sample surface temperatures oscillate inside the measuring error ( $7500 \pm 500$  K). By cooling the sample from  $0^{\circ}\text{C}$  to  $-50^{\circ}\text{C}$ , the calculated electron density is reduced for times and below  $-10^{\circ}$  it is at the order of  $10^{15} \text{ cm}^{-3}$ . A decreasing trend of the electron density with cooling is consistent with the observed increase of  $\text{Mg}^+/\text{Mg}$  ratio at lower sample temperatures (section 3.1). When the lower laser energy density was applied on the sample, on the Boltzmann plot the energy levels corresponding to upper transitions from 3-3.5 eV are clearly under populated, resulting in a virtually higher plasma temperatures (above 8500 K). Such behavior is an indicator of a loss of LTE, as it might be expected for such low electron densities as here.

The observed changes of the plasma electron densities with the sample temperature can strongly affect the calibration and the analytical LIBS accuracy. As for example, we calculated  $\text{Mg}^+/\text{Mg}$  ratio in plasma by applying the Saha equation considering the plasma temperature of 7500 K, for electron densities of  $1 \cdot 10^{16} \text{ cm}^{-3}$  and  $0.5 \cdot 10^{16} \text{ cm}^{-3}$ . In our case, these electron densities correspond to the sample temperatures of  $-10^{\circ}\text{C}$  and  $-30^{\circ}\text{C}$  respectively. Although we cannot consider here the presence of a full LTE, at low electron density the calculated ratio ionic to atomic ratio is twice higher. This indicates an importance of considering the plasma parameters during the calibration whenever the quantitative analyses are required over a wide range of sample temperatures. A method proposed in [31] for quantitative LIBS analyses in presence of variable plasma parameters, deals with the plasma in LTE and can not be applied for plasma with low electron densities as measured here. Consequently, further studies are required to obtain a generally valid calibration in Martian conditions.

#### 4. CONCLUSIONS

LIBS signal from soils/rocks containing structural or surface moisture, at pressures above 6 mbar shows strong temperature dependence below  $0^{\circ}\text{C}$ . We attributed such a signal behavior to the phase transition of supercooled water, present inside small pores and at grain boundaries. The temperature of the freezing of the confined supercooled water depends on the material pore size and roughness. In proximity of the phase transition temperatures, we measured signal depression up to an order of magnitude. The observed LIBS signal loss, whose amount did not change when the laser fluence was increased about three times, can reduce significantly the analytical capability of the technique. Particularly severe signal reduction was registered on

the polished samples, where a narrower pore size distribution was present. On the ice sample, the LIBS signal shows a general decreasing tendency with lowering of the temperature, while at  $-50^{\circ}\text{C}$  it was reduced even for two orders of magnitude. Very small ablation rate of the ice at this temperature can compromise a possibility to remove it from the surface in order to analyze underlying soil/rock material.

Although here described measurements were performed in  $\text{CO}_2$  environment at pressure of 7 mbar, similar effects can be expected in other environments above the triple point, whenever the moisture/ice is present in the sample.

In the temperature range planned for the measurements on Mars ( $+30^{\circ}\text{C}$  to  $-60^{\circ}\text{C}$ ), supercooled water has two transition points, one around  $-40^{\circ}\text{C}$  and another at about  $-50^{\circ}\text{C}$ . On different samples, we registered a depression of LIBS signal close to these temperatures. Another point of the signal depression was always registered on all soil/rock samples in proximity of  $0^{\circ}\text{C}$ , attributed to freezing/melting of hexagonal ice, present inside larger pores or scratches. From these results, it can be suggested that LIBS analysis also in Martian conditions, should exclude the operation close to the points of the known water/ice transitions, i.e. around  $0^{\circ}\text{C}$ ,  $-40^{\circ}\text{C}$  and  $-50^{\circ}\text{C}$ . The larger focal spot size would allow for interaction with a wider range of pore dimensions present on the natural samples, thus to reduce the signal changes with the temperature due to water/ice transitions dependent on the pore size.

This work points out a necessity to further investigate the LIBS signal behavior at subzero temperatures, including the influence of pore size distribution and the degree of moisture. Also, it indicates that the calibration procedure for quantitative analyses should take into account the plasma parameters, being the plasma electron density strongly dependent on the sample temperature.

#### ACKNOWLEDGMENTS

This project was supported by the Deutsches Zentrum für Luft- und Raumfahrt e.V., research project number 50 QX 0602.

#### REFERENCES

1. Jessberger E. K. et al, GENTNER – a miniaturized laser instrument for planetary in-situ analysis, ESA Call for Ideas of the Pasteur instrument payload for Exomars rover mission (submitted to ESA May 2003).
2. Del Bianco A., et al, GENTNER – a miniaturised LIBS/Raman instrument for the comprehensive in situ analysis of the Martian surface, 4th NASA International Planetary Probe Workshop 2006.
3. Jakosky B. M. and Mellon M. T., Water on Mars, *Physics Today*, April, 71-85, 2004.
4. Levrard B., et al, Recent ice-rich deposits formed at high latitudes on Mars by sublimation of unstable

- equatorial ice during low obliquity, *Nature*, Vol. 431, 1072-1075, 2004.
5. <http://www.lsbu.ac.uk/water/sitemap.html>
6. Schreiber A., et al, Melting and freezing of water in ordered mesoporous silica materials, *Phys. Chem. Chem. Phys.*, Vol 3, 1185-1195, 2001.
7. Liu E., et al, Neutron diffraction and NMR relaxation studies of structural variation and phase transformations for water/ice in SBA-15 silica: I. The over-filled case, *J. Of Physics: Cond. Mat.*, Vol. 18, 10009-10028, 2006.
8. Johari G. P., On the coexistence of cubic and hexagonal ice between 160 and 240 K, *Philos. Magazine B*, Vol 78, 375-383, 1998..
9. Debenedetti P. G. and Stanley H. E., Supercooled and glassy water, *Physics Today*, June, 40-46, 2003.
10. Engemann S., et al, Interfacial melting of ice in contact with SiO<sub>2</sub>, *Phys. Rev. Lett.*, Vol. 92, 205701: 1-4, 2004.
11. Dash J. G., et al, The premelting of ice and its environmental consequence, *Rep. Prog. Phys.*, Vol. 58, 115-167, 1995.
12. Watanabe K. and Mizoguchi M., Amount of unfrozen water in frozen porous media saturated with solution, *Cold Reg. Sci., Tech.*, Vol. 34, 103-110, 2002.
13. Fink U. and Larson H., temperature dependence of water-ice spectrum between 1 and 4 micron: application to Europa, Ganymede and Saturn's rings, *ICARUS*, Vol. 24, 411-420, 1975.
14. Slack G. A., Thermal conductivity of ice, *Phys. Rev. B*, Vol. 22, 3065-3071, 1980.
15. Cremers D. A. and Radziemsky L. J., *Handbook of Laser-Induced Breakdown Spectroscopy*, John Wiley&Sons Ltd, (2006)
16. Sallé B., et al, Evaluation of a compact spectrograph for in-situ and stand-off laser-induced breakdown spectroscopy analyses of geological samples on Mars missions, *Spectrochim. Acta Part B*, Vol. 60, 805-815, 2005.
17. Colao F., et al, LIBS application for analyses of martian crust analogues: search for the optimal experimental parameters in air and CO<sub>2</sub> atmosphere, *Appl. Phys. A*, Vol. 79, 143-152, 2004.
18. Wisbrun R., et al, Detector for trace elemental analysis of solid environmental samples by laser plasma spectroscopy, *Anal. Chem.*, Vol. 66, 2964-2975, 1994.
19. Sallé B., et al, Laser-induced breakdown spectroscopy for space exploration applications: influence of the ambient pressure on the calibration curves prepared from soil and clay samples, *Spectrochim. Acta Part B*, Vol. 60, 479-490, 2005.
20. Knight A. K., et al, Characterization of Laser-Induced Breakdown Spectroscopy for application to space exploration, *Appl. Spectrosc.*, Vol. 54, 331-340, 2000.
21. Castle B.C., et al, Variables Influencing the Precision of Laser-Induced Breakdown Spectroscopy Measurements, *Appl.Spectrosc.*, Vol. 52, 649-657, 1998.
22. Eppler A. S., et al, Matrix effects in the detection of Pb and Ba in soils using laser-induced breakdown spectroscopy, *Appl. Spectrosc.*, Vol. 50, 1175-1181, 1996.
23. Sallé B., et al, Comparative studies of different methodologies for quantitative rock analysis by Laser-Induced Breakdown Spectroscopy in a simulated Martian atmosphere, *Spectrochim. Acta Part B*, Vol. 61 301-313, 2006.
24. Arp Z. A., et al, Analysis of water ice and water ice/soil mixtures using laser-induced breakdown spectroscopy: application to Mars exploration, *Appl. Spectrosc.*, Vol. 58, 897-909, 2004.
25. Colao F., et al, Investigation of LIBS feasibility for in situ planetary exploration: An analysis on Martian rock analogues, *Planetary and Space Sci.* Vol. 52, 117-123, 2004.
26. Caceres J. O., et al, Quantitative analysis of trace metal ions in ice using laser induced breakdown spectroscopy, *Spectrochim. Acta Part B*, Vol. 56, 831-838, 2001.
27. Lazic V., et al, Laser Induced Breakdown Spectroscopy in water: improvement of the detection threshold by signal processing, *Spectrochim. Acta Part B*, Vol. 60, 1002-1013, 2005.
28. Bergamn R, et al, Dielectric study of supercooled 2D water in a vermiculate clay, *J. of Chem. Phys.*, Vol. 113, 357-363, 2000.
29. Ito K., et al, Thermodynamic determination of fragility in liquids and a fragile-to-strong liquid transition in water, *Nature*, Vol. 398, 492-495, 1999.
30. Setzer M. J. and Liebrecht A., Frost dilatation and pore system of hardened cement paste under different storage conditions, In *Frost resistance of concrete - From nanostructure and pore solution to macroscopic behavior and testing* (Setzer, M.J. et al.; Eds.) RILEM PRO 24, 169-178, 2002.
31. Lazic V., et al, Quantitative Laser Induced Breakdown Spectroscopy analysis of ancient marbles and corrections for the variability of plasma parameters and of ablation rate, *J. Anal. At. Spectrom.*, Vol. 19, 429-436, 2004.